Nanoscale

Dual Wavelength-Activatable Gold Nanorod Complex for Synergistic Cancer Treatment

Journal:	*Nanoscale*
Manuscript ID:	NR-ART-03-2015-001568.R1
Article Type:	Paper
Date Submitted by the Author:	01-Apr-2015
Complete List of Authors:	Pacardo, Dennis; University of North Carolina at Chapel Hill and North Carolina State University, Joint Department of Biomedical Engineering Neupane, Bhanu; University of North Carolina at Chapel Hill and North Carolina State University, Joint Department of Biomedical Engineering Rikard, S. Michaela; University of North Carolina at Chapel Hill and North Carolina State University, Joint Department of Biomedical Engineering Lu, Yue; University of North Carolina at Chapel Hill and North Carolina State University, Joint Department of Biomedical Engineering Mo, Ran; University of North Carolina at Chapel Hill and North Carolina State University, Joint Department of Biomedical Engineering Mishra, Sumeet; North Carolina State University, Department of Materials Science and Engineering Tracy, Joseph B.; North Carolina State University, Department of Materials Science and Engineering Wang, Gufeng; North Carolina State University, Department of Chemistry Ligler, Frances; North Carolina State University, Biomedical Engineering; UNC-Chapel Hill School of Medicine, Biomedical Engineering Gu, Zhen; University of North Carolina at Chapel Hill,

Nanoscale

RSCPublishing

Paper

Dual Wavelength-Activatable Gold Nanorod Complex for Synergistic Cancer Treatment

Cite this: DOI: 10.1039/x0xx00000x

Dennis B. Pacardo,[a,b] Bhanu Neupane,[a] S. Michaela Rikard,[a] Yue Lu,[a,b] Ran Mo,[a,b] Sumeet R. Mishra,[c] Joseph B. Tracy,[c] Gufeng Wang,[d] Frances S. Ligler [a,*] and Zhen Gu [a,b,e,*]

Received 10th March 2015,
Accepted 00th March 2015

DOI: 10.1039/x0xx00000x

www.rsc.org/nanoscale

A multifunctional gold nanorod (AuNR) complex is described with potential utility for theranostic anticancer treatment. The AuNR was functionalized with cyclodextrin for encapsulation of doxorubicin, with folic acid for targeting, and with a photo-responsive dextran-azo compound for intracellular controlled drug release. Interaction of AuNR complex toward HeLa cells was facilitated via the folic acid targeting ligand as displayed in the dark-field images of cells. Enhanced anticancer efficacy was demonstrated through synergistic combination of promoted drug release upon ultraviolet (UV) light irradiation and photothermal therapy upon infrared (IR) irradiation. This multifunctional AuNR-based system represents a novel theranostic strategy for spatiotemporal delivery of anticancer therapeutics.

1. Introduction

Recent advances in nanotechnology have made significant contributions in the development of novel materials, which can be tailored and functionalized for broad applications in cancer research.[1-8] For example, nanocarriers can accumulate in tumor sites through the enhanced permeability and retention (EPR) effect that can be exploited for co-delivery of therapeutic drugs and diagnostic agents in a single formulation. Such a theranostic combination provides for simultaneous drug delivery, imaging and monitoring of treatment response.[9, 10] Conveniently, inorganic nanomaterials such as quantum dots,[11-13] iron oxide nanoparticles,[14-16] carbon nanotubes,[17] silica nanoparticles[18,19] and gold nanoparticles/nanorods,[20-24] have been extensively employed as imaging agents; while their well established synthesis and surface functionalization can be followed by loading of therapeutic agents and conjugation of targeting moieties, with consequent increases in intracellular uptake. Moreover, these nanomaterials can be loaded with two or more therapeutic agents and programmed for site-specific delivery and stimuli-triggered drug release for enhanced efficacy.[25-29] While the properties of these inorganic nanomaterials offer a lot of advantages and promises, concerns and limitations such as cytotoxicity, biocompatibility, cost and selectivity are critical hurdles to their advancements in clinical trials.[10] However, gold-based nanomaterials have been found to be inherently non-cytotoxic,[30-34] thus attracting significant interest for cancer therapeutics.

In theranostic nanomedicine, gold-based nanomaterials have been widely studied due to their light scattering properties which are suitable for imaging applications and ease of surface functionalization which simplifies ligand attachment and anticancer drug conjugation.[9, 10, 35, 36] Gold nanomaterials also have characteristic surface plasmon resonance that can be employed for localized light-induced heating sufficient to produce cell death by hyperthermia.[37, 38] Early studies of theranostic gold nanomaterials reported by El-Sayed and co-workers employed gold nanorods (AuNR) conjugated to monoclonal antibodies specific for epidermal growth factor receptor (anti-EFGR) for imaging and photothermal therapy (PTT) of neoplastic oral epithelial cell lines.[39] In this system, dark-field microscopy was used for cancer cell imaging;[39] however, other imaging techniques were later developed. For example, two-photon imaging used silica-coated AuNR as contrast agents[40] and surface-enhanced Raman scattering (SERS) used AuNRs tagged with Raman probes.[41] For the therapeutic application of AuNRs, PTT was achieved by irradiation using IR light in accordance with the longitudinal SPR associated with the rods. Exposure of AuNRs to IR light causes rapid temperature increase that can reach the threshold (41 - 43 °C)[42] for hyperthermia-induced cancer cell apoptosis.[37] Moreover, IR light penetrates deeply into tissues, which can be exploited for on-demand local heating of tumors.[43] Furthermore, functionalization of the AuNR surface can be used to attach ligands for anticancer drug encapsulation and intracellular delivery.[41, 44-46] The combined drug delivery and PTT effects of AuNRs showed higher killing efficiency for cancer cells, while the addition of imaging and detection functions generate the potential for targeted delivery and monitoring of therapeutic efficacy.[47, 48] However, limitations such as low drug loading capacity, dose-induced toxicity and detection sensitivity remained to be addressed to fully realize the potential of AuNRs for cancer theranostics.

In this research, we developed a multifunctional AuNR complex, illustrated in **Fig. 1a**, composed of three main components: 1) cyclodextrin-functionalized AuNR for drug encapsulation, 2) dextran-4-phenyl-azo-benzoate (DexAzo) as a capping agent and 3) folic acid-PEG-maleimide-adamantane (FA) as targeting component. The cyclodextrin moiety in AuNR encapsulates small drug molecules such as doxorubicin (DOX)[49, 50] and adamantane[51-53] in its hydrophobic core forming a guest-host inclusion complex, thereby providing drug delivery and cancer cell targeting functions. In addition, the DexAzo compound serves as capping / uncapping agent due to

the trans-cis isomerization of the azo moeity upon UV irradiation, providing triggered drug release.[54] In combination with the drug delivery function, IR light treatment induces intracellular hyperthermia via PTT which contributes to cancer cell death. Moreover, the inherent ability of AuNR for light scattering was exploited for imaging applications via dark-field microscopy. This multifunctional AuNR complex has the potential to constitute a new approach for cancer therapy that illuminated targeted cells two independent wavelengths of light for increased toxicity control, as shown in **Fig. 1b**. The multifunctional AuNR complex demonstrated excellent biocompatibility and novel UV and IR light activated synergistic effects for inducing apoptosis in cancer cells.

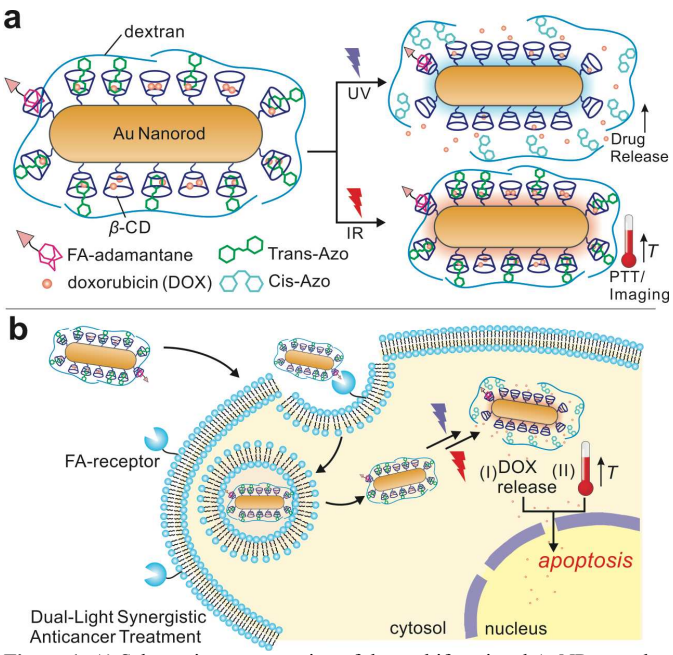

Figure 1. A) Schematic representation of the multifunctional AuNR complex for UV-triggered drug delivery and IR-induced photothermal therapy (PTT) and cell imaging. B) Intracellular delivery of the AuNR complex and the dual-light synergistic effects of DOX release and hyperthermia resulting in apoptosis.

2. Materials and Methods

2.1 Materials

Cetyltrimethylammonium bromide (CTAB), $HAuCl_4 \bullet 3H_2O$, 11-mercaptoundecanoic acid (MUA), (2-hydroxypropyl)-β-cyclodextrin (CD), N,N'-dimethylformamide (DMF), N,N'-dicyclohexylurea (DCC), hexadeuterodimethyl sulfoxide (d_6-DMSO), dichloromethane (DCM), dimethyl sulfoxide (DMSO), dextran from Leuconostoc mesenteroides (MW 35K – 40K), 4-phenyl-azo-benzoic acid, N,N'-carbonyldiimidazole (CDI) and 1-adamantanethiol were obtained from Sigma-Aldrich. $NaBH_4$, $AgNO_3$, L-ascorbic acid, ethanol (EtOH) were purchased from Fisher Scientific while 4-dimethylaminopyridine (DMAP) was obtained from Acros Organics. Doxorubicin hydrochloride (DOX) was obtained from BIOTANG Inc. (Lexington, MA, USA). Folic acid-PEG-maleimide (MW 2000) was purchased from Nanocs, Inc. (New York, NY) while trypan blue was obtained from HyClone Laboratories (Logan, UT).

2.1 Synthesis and Characterization of AuNRs

The AuNRs were synthesized using a seed-mediated method, which was previously reported.[55, 56] Briefly, gold nanoparticle (AuNP) seeds were first synthesized in CTAB solution (7.5 mL, 100 mM) by adding the gold metal precursor, $HAuCl_4 \bullet 3H_2O$ (Au^{3+}) (250 µL, 10 mM) with cold $NaBH_4$ solution (600 µL, 10 mM). After 1 h of incubation, the AuNP seeds (210 µL) were then added to a growth solution composed of the following: Au^{3+} (2.0 mL, 10 mM), CTAB (47.5 mL, 100 mM), $AgNO_3$ (300 µL, 10 mM) and ascorbic acid (320 µL, 100 mM), to generate CTAB-AuNRs. Excess CTAB was removed from the CTAB-AuNRs solution by centrifugation. The washing process was done twice and the purified CTAB-AuNR was redispersed in deionized water. Functionalization of CTAB-AuNR (**Fig. S1**) was then performed through ligand exchange with MUA (10 mM) in 50:50 EtOH:H_2O solution. Equal amounts (25 mL) of CTAB-AuNR and MUA solution were mixed overnight in a rotating wheel.[57] The resulting MUA-AuNR was washed twice with water to remove excess CTAB and MUA and the precipitate was redispersed in DMF for further functionalization. The CD (720 mg) was then added to MUA-AuNR (50 mL) in DMF to facilitate the coupling reaction in the presence of DCC (210 mg) and DMAP (125 mg) as base at room temperature for 24 h.[50] After the synthesis, the CD-AuNR was isolated through centrifugation, washed with water and filtered using PVDF 45-µm filter (Fisherbrand) to remove excess DCC. Further purification was done by dialyzing the CD-AuNR against water using a dialysis membrane with MWCO of 12K. The filtered and dialyzed CD-AuNR samples were then refrigerated for future use.

In each step of the synthesis of AuNRs, characterization techniques were employed to verify the functionalization procedure. UV-vis analysis was done by absorbance scan from 300 to 1000 nm using Tecan Infinite M200 Pro multiplate reader. Sample preparation for transmission electron microscopy (TEM) analysis was done by applying a drop of AuNR solution in copper grid (Ted Pella) and air-dried at room temperature overnight. TEM imaging was then accomplished using JEOL 2000FX S/TEM operated at 200kV with LaB_6 as electron source. To characterize the surface functionalization of AuNRs, ^{1}H NMR analysis was performed using 300 MHz Varian Gemini instrument with dried samples dissolved in d_6-DMSO and placed in NMR tube. FTIR analysis was done using ThermoElectron FTIR with samples dissolved in DCM. Solution based size and zeta potential analysis were performed using a Zetasizer Nano System (Malvern).

2.3 Synthesis of photoactive dextran-4-phenyl-azo-benzoate (DexAzo) and targeting ligand, folic acid-PEG-maleimide-adamantane (FA)

The DexAzo complex was synthesized by dissolving dextran (500 mg) and 4-phenyl-azo-benzoic acid (679 mg), in DMSO (15.0 mL) (**Fig. S3a**). Upon addition of CDI (487.5 mg), the reaction was heated to 80 °C and allowed to proceed for 20 h with constant stirring. The product was precipitated and washed with EtOH and dried under vacuum. ^{1}H NMR analysis was done to characterize the final product. The targeting ligand, on the other hand, was synthesized by coupling commercially available folic acid-PEG-maleimide (MW 2000) (500 µL, 10 mg/mL) with 1-adamantanethiol (500 µL, 5 mg/mL) in DMSO at room temperature with constant stirring for 24 h. The product, FA, was then placed in dialysis membrane to remove unreacted starting materials.

2.3 DOX encapsulation and UV-triggered release

For encapsulation of DOX, CD-AuNR (500 μL, 0.09 nM) was mixed with DOX solution (20 μL, 5 mg/mL) and targeting ligand (10 μL) using a vortexer. Afterwards, DexAzo (100 μL, 1 mg/mL) was added and the solution was incubated in the dark for 24 h in a rotating wheel at room temperature. The DOX-loaded CD-AuNR with DexAzo and targeting ligand was then separated by centrifugation, washed with water, isolated and stored at 4 °C for future use. For drug release studies, the DOX-loaded CD-AuNR was added with 1 mL deionized water and irradiated with UV light using Dymax BlueWave 75 UV lamp. Aliquots of the sample (20 μL) were collected before and after irradiation to monitor DOX release using fluorescence scanning measurements. Different irradiation times were used to determine the least amount of time needed for optimum DOX release. The fluorescence scan was plotted to show the increase in fluorescence in the medium after UV treatment to show DOX release (Fig. S5). The fluorescence intensity at 595 nm was then use to plot the DOX release profiles.

2.4. Dark field imaging applications for functionalized AuNRs.

HeLa cells (1 x 10^5 cells/well) were cultured in glass slides placed in 6-well plates for 24 h. AuNR formulations (2.0 mL), with FA (FA-CD-AuNR) and without FA (CD-AuNR) in culture media were then incubated with HeLa cells on glass slide. After 4 h of incubation, the cells were imaged using a Nikon eclipse 80i microscope equipped with Andor camera with dark-field condenser (oil 1.43 – 1.2 NA) and 100x (oil 1.5 – 1.25) objective.

2.5 Cell viability studies

HeLa cells (1 x 10^5 cell/well) were seeded in 96-well plate and cultured using DMEM with fetal bovine serum (10% (v:v)), penicillin (100U/ml) and streptomycin (100 mg/ml) in an incubator at 37 °C under an atmosphere of 5% CO_2 and 90% relative humidity. Different formulations of DOX-loaded CD-AuNRs (equivalent to DOX concentrations of 0.25, 0.5, 1.0, 2.0 and 4.0 μM) were then incubated with HeLa cells for 4 h, after which the solution was removed and replaced with fresh DMEM culture media. The cells were then subjected to 5 s of UV irradiation using Dymax BlueWave 75 UV lamp. The cells were then incubated for 24 h, followed by the standard MTT assay for cell viability. Similarly, control experiments were performed for cell viability studies employing the same protocol but with the following formulations: DOX-loaded CD-AuNR without UV, CD-AuNR with and without UV and standard DOX solutions.

2.6 Photothermal Therapy Application of AuNRs

IR irradiation was initially performed to a 2.0 mL solution of CD-AuNR using a red laser at 800 nm at 1.5 W/cm^2 power for 12 min. The increase in solution temperature was monitored using a digital thermometer. HeLa cells (in glass slides, prepared as described above) were incubated with CD-AuNRs for 4 h as described above. The glass slides were then marked with several small circular spots to indicate the section where the laser was focused for 10 minutes. Afterwards, the cells were stained with trypan blue to visually observe the dead cells. Nikon Eclipse Ti bright field microscope equipped with a Tucsen colored camera was utilized to get the cell images after irradiation and typan blue incubation.

2.7 Confocal Laser Scanning Microscopy (CLSM)

HeLa cells (1 x 10^5 cells/well) in DMEM culture media were seeded in confocal dish and then incubated with DOX-loaded FA-CD-AuNR-DexAzo at different time points: 4 h, 2, h, 1 h and 0.5 h. After the incubation period, the cells were washed with PBS (2 mL, 3x) and then stained with 1 mL of LysoTracker Green solution (1 μL in 20 mL FBS-free DMEM). The cells were then incubated at 37 °C for 0.5 h then washed with PBS (2 mL, 3x). Addition of 1 mL of Hoechst 33342 solution (1 μL in 10 mL FBS-free DMEM) was then performed and the cells were incubated for 10 min. After which, the cells were washed with PBS (2 mL, 3x) and added with 0.5 mL DMEM culture media. Confocal images for each time point (Fig. S7) were then obtained using Zeiss LSM710 confocal microscope.

2.8 Synergistic Effects

HeLa cells (1 x 10^5 cells/well) in DMEM culture media were seeded in confocal dish and then incubated with DOX-loaded FA-CD-AuNR-DexAzo for 4 h. The culture media was then replace with a fresh solution then the right half of the confocal dish was covered with aluminum foil to prevent exposure from UV and IR irradiation. The cells in the left half of the confocal dish was then subjected to 5 s UV and 10 min IR treatment. After this, the cells were washed with PBS (2 mL, 3x) then incubated with 150 μL LIVE/DEAD assay solution (composed of 20 μL EthD-1 stock solution added with 5 μL calcein AM stock solution in 10 mL PBS) for 0.5 h. The cells were then viewed using fluorescence microscope monitoring the green fluorescence of live cells (ex/em, 495 nm/515 nm) and the bright red fluorescence in dead cells (ex/em, 495 nm/635 nm).

3. Results and Discussion

The functionalized AuNR were synthesized using the seed-mediated method[55, 56] with CTAB as a stabilizer, followed by a ligand-exchange reaction with MUA.[57] Next, the coupling reaction between the carboxylic acid group of MUA and the hydroxy group of CD[50] generated CD-AuNRs (Fig. S1 and S2). Initial characterization after functionalization was performed using UV-vis analysis as shown in **Fig. 2a**. Two distinct absorbance peaks were observed at 510 nm and 800 nm, which correspond to the transverse and longitudinal surface plasmon resonances, respectively. TEM images (**Fig. S2b**) showed the formation of nearly monodispersed nanorods with an aspect ratio of around 3.7, which was conserved during functionalization. Dynamic light scattering analysis showed that CD-AuNRs have an average size of 99 ± 10 nm and a zeta potential of -20 ± 1 mV. The CD component can encapsulate small molecules such as DOX and can also interact with the trans isomer of the azo moeity in its hydrophobic core. Exploiting these interactions, DexAzo was then synthesized via direct coupling reaction between dextran and 4-phenyl-azo-benzoic acid (**Fig. S3**).[58]

The DexAzo component then serves as capping agent for CD-AuNR, forming a thin membrane layer that fully encapsulates the AuNRs as shown in the TEM image (**Fig. 2b**). The phenyl-azo moeity of the DexAzo undergoes trans to cis isomerization in the presence of UV light;[54] thereby triggered drug release can be accomplished. To demonstrate this function, DOX was encapsulated in CD-AuNR after 24 h incubation together with DexAzo with a loading capacity of 0.23 mM per 0.5 mL CD-AuNR (**Fig. S4b**). The DOX-loaded CD-AuNR-DexAzo complex was then redispersed in

deionized water and exposed to UV light for 5 s, 10 s and 30 s; after which the increase in DOX levels was monitored using fluorescence intensities (I_t) at 595 nm of the aliquots taken at 5, 10, 20 and 30 min after UV treatment. The ratio of fluorescence intensities, I_t/I_0 (I_0: initial fluorescence intensity before irradiation), was then plotted with time (**Fig. 2c**). The increase in fluorescence intensity at 595 nm due to DOX release after defined time interval was clearly demonstrated in the representative fluorescence spectra shown in **Fig. S5**. With 30 s of UV treatment, the fluorescence intensity due to DOX increased to about 1.9 times the initial value (**Fig. 2c**, pink plot) signifying the release of the drug from CD-AuNR-DexAzo complex due to the isomerization of the azo component. The DOX fluorescence intensity ratios were also maintained between 1.9 and 2.1 throughout the duration of the analysis. In order to find the optimum DOX release conditions at a shorter irradiation time, the analysis was carried out using 10 s and 5 s of UV exposure. While not quite as much DOX was released for the shorter irradiation time as for that of 30 s exposure, the results in **Fig. 2c**, show that, as with the 30 s exposure, most of the DOX release was complete after the first irradiation. Thus in further studies, 5 s UV irradiation was used as the exposure time. Furthermore, results of the control studies showed that no significant increase in fluorescence intensity ratios was observed for the system without UV irradiation, indicating the importance of the capping agent for drug release. As a control experiment, UV treatment of the DOX loaded CD-AuNR without DexAzo did not result in DOX release as shown in **Fig. 2c** (green plot) signifying that UV exposure did not promote DOX release. Taken together, the uncapping of DexAzo upon UV irradiation can effectively promote release of DOX cargo from CD.

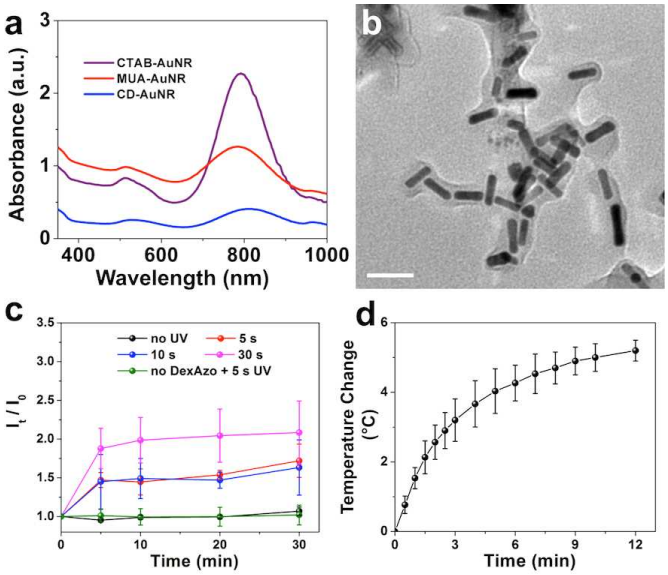

Figure 2. A) Characterization of AuNRs after each functionalization step using UV-vis analysis. B) TEM image of CD-AuNR-DexAzo complex showing full encapsulation of the rods by DexAzo (scale bar = 50 nm). C) The UV-triggered drug release from DOX-loaded CD-AuNR-DexAzo was evaluated at different irradiation times (0, 5, 10 and 30 s) and monitored using DOX fluorescence scanning at 0, 5, 10, 20 and 30 min after irradiation. Error bars indicate the mean ± SD (n = 3). D) The IR-induced hyperthermia of CD-AuNR-DexAzo complex was monitored by direct temperature measurement using digital thermometer. The nanorods solution was heated to 37 °C prior to laser irradiation. Error bars indicate the mean ± SD (n = 3).

Next, the nanomaterials were exposed to IR light to determine their potential for photothermal therapy. In this case, an aqueous solution of the complex was placed in a glass vial and irradiated with a red laser at 800 nm[59] which corresponds to the longitudinal surface plasmon resonance of AuNR.[39] Exposure of the rods to IR light at 800 nm at 1.5 W/cm^2 causes collective oscillation of surface electrons which in turn resulted in localized heating phenomenon. In cancer research, this property of gold nanomaterials has been used to induce cell death by hyperthermia, typically by inducing temperatures between 41 and 43 °C.[42] To mimic the temperature change under biological conditions, the AuNRs were heated to a starting temperature of 37 °C using a heat gun before laser exposure.[59] The temperature change of the system was then measured using a digital thermometer and the results were plotted in **Fig. 2d**. An average temperature change of 5 °C was determined after 10 min of laser irradiation, indicating the capability of the CD-AuNR-DexAzo complex for photothermal therapy in cancer cells.[37, 42]

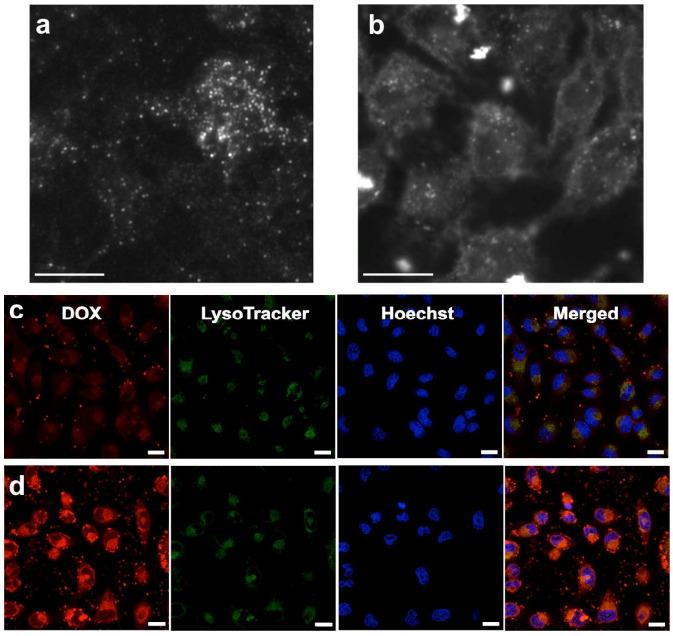

Figure 3. In vitro studies using HeLa cells. Dark-field images of HeLa cells incubated with AuNR-DexAzo complex for 4.0 h at 37 °C: A) without FA targeting ligand and B) with FA targeting ligand (Scale bars: 10 μm). Intracellular delivery of DOX in HeLa cells was observed using confocal laser scanning microscope (CLSM) after incubation with DOX-loaded FA-CD-AuNR-DexAzo at 37 °C for C) 0.5 h and D) 4.0 h (Scale bars: 20 μm). The cells were stained by LysoTracker Green solution for 30 min and Hoechst 33342 solution for 10 min prior to CLSM imaging.

In order to equip the CD-AuNR complex with targeting capability in cancer therapy, a folic acid-based ligand was synthesized using a folic acid-PEG-maleimide compound reacted with adamantane thiol in DMSO. By this method, the straightforward thiol-maleimide "Click" reaction[60, 61] was exploited to attach the adamantane group into the folic acid-terminated moiety to produce the targeting ligand, FA. Upon incubation of FA with CD-AuNR and DexAzo, the adamantane component was inserted into the CD core and served as anchor for the folic acid moiety, generating FA-CD-AuNR-DexAzo. The long PEG spacer chain ensured that the targeting group was exposed upon the DexAzo coating in order to interact effectively with cancer cells bearing folic acid receptors.[62-64] To validate the targeting capability of FA, HeLa cells were incubated separately with FA-CD-AuNR-DexAzo and CD-AuNR-DexAzo. After 4 h of incubation, images of the cells were taken using a dark-field microscope. This technique exploits the ability of AuNRs to strongly scatter white light (350 – 900 nm)[39] to produce a dark-field image of HeLa cells. The results of the

imaging experiment, shown in **Fig. 3a-b**, clearly demonstrate the effect of FA on the interaction and selectivity of AuNR complex in cancer cells. For the cells incubated without the targeting ligand (**Fig. 3a**), the rods were randomly distributed and the cells were not clearly imaged. In contrast, the cytoplasm of HeLa cells incubated with FA loaded AuNR complex was clearly visible as a result of the interaction between the targeting ligand and the folic acid receptors (**Fig. 3b**). The dark-field imaging experiments showed the importance of FA as a targeting ligand moiety for selectivity and specificity of the cancer cell recognition.

Next, HeLa cells were incubated with a DOX-loaded FA-CD-AuNR-DexAzo complex for 4.0 h at 37 °C. After 5 s of UV treatment, the intracellular delivery of DOX was monitored by CLSM at different time points. The fluorescence of DOX was clearly observed after 0.5 h of incubation which indicates effective internalization of drug carriers (**Fig. 3c**). When the incubation time was extended to 4 h, the fluorescence signal of DOX was displayed inside the nucleus as demonstrated by the magenta color in the merged image (**Fig. 3d**), indicating the combined fluorescence of the Hoechst-stained nucleus and DOX. The results of these in vitro studies clearly demonstrate the capability of the AuNR complex as drug delivery vehicle in HeLa cells.

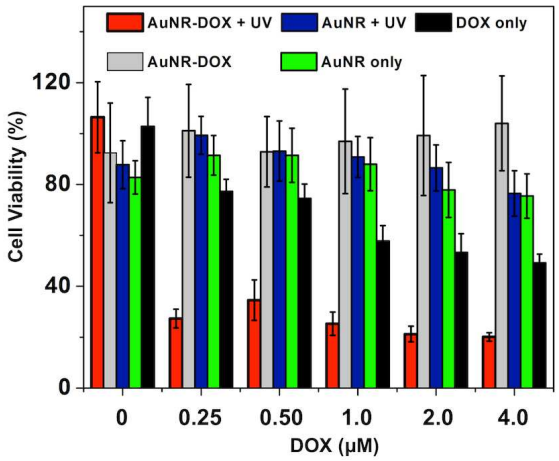

Figure 4. Cell viability studies using HeLa cells as model system for intracellular drug delivery of the multifunctional AuNR complex. HeLa cells were incubated with different formulations of the DOX-loaded AuNR complex and control systems. Error bars indicate the mean ± SD (n = 5).

In order to determine the efficiency of intracellular DOX delivery and release from the AuNR complex, a cell viability study was performed using the MTT viability assay. For comparison, standard solutions of DOX were also incubated with HeLa cells as well as controls containing DOX-free AuNR complex. After addition of different formulations to HeLa cells, the culture was incubated for 4 h at 37 °C prior to 5 s UV irradiation. The cells were then further incubated for 24.0 h, and then MTT assay was performed. As shown in **Fig. 4**, the DOX-loaded FA-CD-AuNR-DexAzo complex (**Fig. 4**, red bars) caused a decrease in cell survival to 27 ± 4% for the least concentrated formulation (0.25 μM DOX). As the amounts of DOX-loaded AuNR complex increased, HeLa cell viability correspondingly decreased, down to 20 ± 2% for 4.0 μM DOX, which is remarkably lower viabilities after exposure to control solutions of DOX (**Fig. 4**, black bars). These results can be attributed to a more efficient intracellular uptake of DOX-loaded AuNRs through receptor-mediated endocytosis compared with free DOX solution. Furthermore, results of control reactions suggest that 5 s UV irradiation showed negligible effect on the cell survival. Additionally, results of the DOX-loaded AuNR complex without UV irradiation (**Fig. 4**, gray bars), showed insignificant toxicity toward HeLa cells, suggesting that no significant DOX release occurred in the absence of the UV trigger. When DOX-free nanorods were incubated with HeLa cells and exposed to UV light, the assay results (**Fig. 4**, blue bars) showed viability of approximately 90%, for all nanorod formulations, indicating low cytotoxicity from the materials in the AuNR complexes. Similarly, when the formulations containing FA-CD-AuNR-DexAzo were incubated with HeLa cells without UV treatment, no significant decrease in cell viability was observed (**Fig. 4**, green bars). The results of the MTT cell viability assay suggest the efficient intracellular delivery of DOX-loaded AuNR complexes and subsequent UV-activated drug release.

To assess the photothermal efficacy of the AuNR complex, IR irradiation was explored using a red laser at 800 nm at 1.5 W/cm^2 power. The cells were cultured on glass slides and incubated with the AuNR complexes for 4 h prior to 10 min IR exposure. To qualitatively observe the effect of laser treatment on cell survival, trypan blue was used to stain the slides after irradiation. The results (**Fig. S6**) of photothermal irradiation showed that for HeLa cells incubated with AuNR complex, accumulation of trypan blue dye was evident on the spot where the laser was focused indicating cell death by hyperthermia. In contrast, the cells outside the laser spot remained viable. In sharp contrast, control experiments using only HeLa cells showed no accumulation of trypan blue for the cells treated with laser.

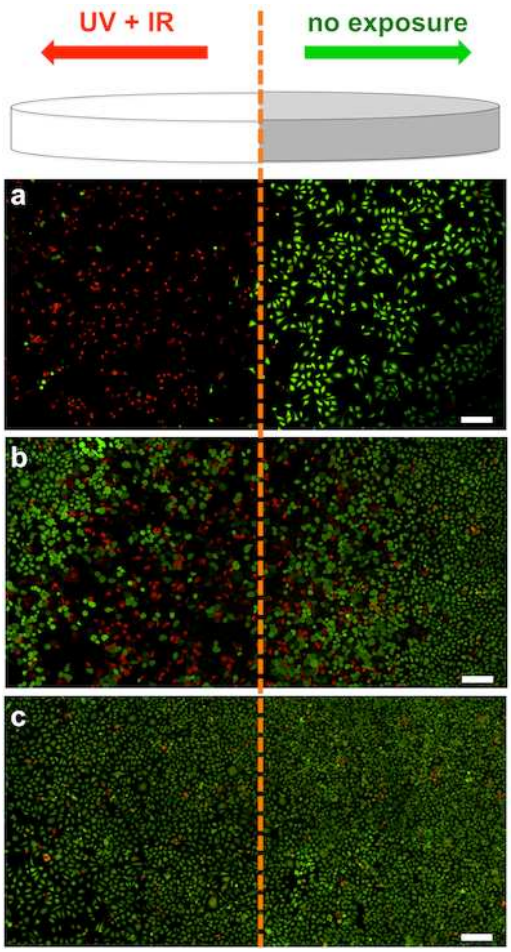

Figure 5. Schematic diagram of the localized UV and IR irradiation to trigger the synergistic effects of DOX release and PTT. The right half of the confocal dish is covered with aluminum foil (no exposure) while the left half

was exposed to UV and/or IR treatment. Fluorescence microscopy images of live (green) and dead (red) HeLa cells after incubation with DOX-loaded AuNR-DexAzo complex for 4.0 h at 37 °C and exposed to A) UV and IR lights, B) IR light only and C) UV light only. Scale bars: 200 μm.

To demonstrate the synergistic effects of UV and IR treatment of multifunctional AuNR complex, the HeLa cells were incubated with the DOX-loaded formulation in confocal dish for 4.0 h at 37 °C. Thereafter, the cells were divided into two zones; the right half was covered with aluminum foil (no UV or IR exposure) while the left half was exposed to 5 s UV and 10 min IR laser treatments (**Fig. 5**). A live-dead cell assay[65] was used to visualize the viability of HeLa cells via fluorescence microscopy wherein a bright red fluorescence from ethidium homodimer-1 indicates dead cells while an intense green fluorescence from polyionic dye calcein indicates live cells. The results (**Fig. 5a**) showed that for HeLa cells incubated with DOX-loaded FA-CD-AuNR-DexAzo and then treated with both UV and IR lights, bright red fluorescence predominates, indicating the presence of dead cells. In contrast, the cells in the right panel remained viable as shown by the intense green fluorescence. As a control system, HeLa cells incubated with DOX-loaded FA-CD-AuNR-DexAzo, were exposed separately with IR or UV only. As shown in **Fig. 5b & c**, minimal dead cells were observed after IR and UV exposure, respectively; although there were some dead cells at the boundary of the unexposed region of **Fig. 5b,** which can be attributed to heat diffusion. Taken together, the synergistic effect of UV and IR irradiation on the DOX-loaded AuNRs increases anticancer therapeutic impact, indicating the potential for spatiotemporal drug delivery and photothermal therapy.

Conclusions

In summary, we have developed a multifunctional AuNR complex with diagnostic function through dark-field imaging and synergistic drug delivery and photothermal therapy induced using two distinct wavelengths of light. The surface functionalization of the AuNRs with CD provide a mechanism for encapsulating DOX with high efficiency and for attaching a targeting ligand which ensures intracellular uptake and drug delivery to the cancer cells. Meanwhile, the combined effects of UV-triggered DOX release and IR-induced hyperthermia show enhanced therapeutic efficacy against cancer cells with spatiotemporal control. Furthermore, the imaging applications of the AuNR complex provide the potential for simultaneous cancer detection and treatment in a single formulation. Taken together, the straightforward synthetic protocol, high drug loading capacity, light-activated drug release and PTT, and dark-field diagnostics of the multifunctional AuNR complex demonstrate a promising new approach for cancer theranostics.

Acknowledgements

This work was supported by the start-up funds provided by the Joint Department of Biomedical Engineering at University of North Carolina - Chapel Hill and North Carolina State University to Prof. Ligler and Prof. Gu. This project was also supported by the Research Innovation Seed Fund from NC State awarded to Prof. Wang, Prof. Ligler and Prof. Gu, the grant 550KR51307 from NC TraCS to Prof. Gu and the National Science Foundation grant DMR-1056653 to Prof. Tracy The authors also acknowledge the use of the Analytical Instrumentation Facility (AIF) at the North Carolina State University, which is supported by the State of North Carolina and the National Science Foundation.

Notes and references

[a] Joint Department of Biomedical Engineering, University of North Carolina at Chapel Hill and North Carolina State University, 911 Oval Dr., Campus Mailbox 7115, Raleigh, North Carolina 27695 USA.
[b] Center for Nanotechnology in Drug Delivery and Division of Molecular Pharmaceutics, UNC Eshelman School of Pharmacy, University of North Carolina at Chapel Hill, Chapel Hill, NC 27599, USA.
[c] Department of Materials Science and Engineering, North Carolina State University, Raleigh, North Carolina 27695 USA.
[d] Department of Chemistry, North Carolina State University, Raleigh, North Carolina 27695 USA.
[e] Department of Medicine, University of North Carolina at Chapel Hill, Chapel Hill, NC 27599, USA.

* Corresponding authors' emails: fsligler@ncsu.edu, zgu@email.unc.edu

Electronic Supplementary Information (ESI) available. See DOI: 10.1039/b000000x/

1. E. K.-H. Chow, D. Ho, *Science Trans. Med.* **2013,** *5*, 216rv4.
2. M. E. Davis, Z. Chen, D.M. Shin, *Nat. Rev. Drug Discovery* **2008,** *7*, 771.
3. O.C. Farokhzad, R. Langer, *ACS Nano* **2009,** *3*, 16.
4. M. Ferrari, *Nat. Rev. Cancer* **2005,** *5*, 161.
5. P. Ghosh, G. Han, M. De, C.K. Kim, V.M. Rotello, *Adv. Drug Delivery Rev.* **2008,** *60*, 1307.
6. G. A. Hughes, *Nanomedicine: NBM* **2005,** *1*, 22.
7. D.B. Pacardo, F.S. Ligler, Z. Gu, *Nanoscale* **2015,** *7*, 3381.
8. D. Peer, J.M. Karp, S. Hong, O.C. Farokhzad, R. Margalit, R. Langer, *Nat. Nanotechnol.* **2007,** *2*, 751.
9. K. Y. Choi, G. Liu, S. Lee, X. Chen, *Nanoscale* **2012,** *4*, 330.
10. J. Xie, S. Lee, X. Chen, *Adv. Drug Delivery Rev.* **2010,** *62*, 1064.
11. V. Bagalkot, L. Zhang, E. Levy-Nissenbaum, S. Jon, P.W. Kantoff, R. Langer, O.C. Farokhzad, *Nano Lett.* **2007,** *7*, 3065.
12. A. M. Smith, H. Duan, A. M. Mohs, S. Nie, *Adv. Drug Delivery Rev.* **2008,** *60*, 1226.
13. P. Zrazhevskiy, M. Sena, X. Gao, *Chem. Soc. Rev.* **2010,** *39*, 4326.
14. M. Das, D. Mishra, P. Dhak, S. Gupta, T.K. Maiti, A. Basak, P. Pramanik, *Small* **2009,** *5*, 2883.
15. J. R. McCarthy, R. Weissleder, *Adv. Drug Delivery Rev.* **2008,** *60*, 1241.
16. H. Xu, L. Cheng, C. Wang, X. Ma, Y. Li, Z. Liu, *Biomaterials* **2011,** *32*, 9364.
17. K. Kostarelos, A. Bianco, M. Prato, *Nat. Nano* **2009,** *4*, 627.
18. J. Kim, H.S.Kim, N. Lee, T. Kim, H. Kim, T. Yu, I.C. Song, W.K. Moon, T. Hyeon, *Angew. Chem., Int. Ed.* **2008,** *47*, 8438.
19. E. Tasciotti, X. Liu, R. Bhavane, K. Plant, A.D. Leonard, B.K. Price, M.M.-C. Cheng, P. Decuzzi, J.M. Tour, F. Robertson, M. Ferrari, *Nat. Nano* **2008,** *3*, 151.
20. E. Boisselier, D. Astruc, *Chem. Soc. Rev.* **2009,** *38*, 1759.
21. L.Y.T. Chou, W.C.W. Chan, *Adv. Healthcare Mater.* **2012,** *1*, 714.
22. D.A. Giljohann, D.S. Seferos, W.L. Daniel, M.D. Massich, P.C. Patel, C.A. Mirkin, *Angew. Chem., Int. Ed.* **2010,** *49*, 3280.
23. C. Wang, J. Li, C. Amatore, Y. Chen, H. Jiang, X.-M. Wang, *Angew. Chem., Int. Ed.* **2011,** *50*, 11644.
24. C. Zhou, G. Hao, P. Thomas, J. Liu, M. Yu, S. Sun, O.K. Öz, X. Sun, J. Zheng, *Angew. Chem., Int. Ed.* **2012,** *51*, 10118.
25. J. Bergh, I.M. Bondarenko, M.R. Lichinitser, A. Liljegren, R. Greil, N. L. Voytko, A.N. Makhson, J. Cortes, A. Lortholary, J. Bischoff, A. Chan, S. Delaloge, X. Huang, K.A. Kern, C. Giorgetti, *J. Clin. Oncol.* **2012,** *30*, 921.
26. T. Jiang, R. Mo, A. Bellotti, J. Zhou, Z. Gu, *Adv. Funct. Mater.* **2014,** *24*, 2295.
27. T.-M. Sun, J.-Z. Du, Y.-D. Yao, C.-Q. Mao, S. Dou, S.-Y. Huang, P.-Z. Zhang, K.W. Leong, E.-W. Song, J. Wang, *ACS Nano* **2011,** *5*, 1483.
28. Y. Lu, W. Sun, Z. Gu, *J. Control. Release* **2014,** *194*, 1.
29. T. Jiang, W. Sun, Q. Zhu, N. A, Burns, S. A. Khan, R. Mo, Z. Gu, *Adv. Mater.* **2015,** *27*, 1021.

30. L.Y.T. Chou, K. Zagorovsky, W.C.W. Chan, *Nat. Nano* **2014,** *9*, 148.
31. E.C. Dreaden, A.M. Alkilany, X. Huang, C.J. Murphy, M.A. El-Sayed, *Chem. Soc. Rev.* **2012,** *41*, 2740.
32. X. Huang, S. Neretina, M.A. El-Sayed, *Adv. Mater.* **2009,** *21*, 4880.
33. N. Lewinski, V. Colvin, R. Drezek, *Small* **2008,** *4*, 26.
34. R. Shukla, V. Bansal, M. Chaudhary, A. Basu, R.R. Bhonde, M. Sastry, *Langmuir* **2005,** *21*, 10644.
35. R. Bardhan, S. Lal, A. Joshi, N.J. Halas, *Acc. Chem. Res.* **2011,** *44*, 936.
36. M.P. Melancon, M. Zhou, C. Li, *Acc. Chem. Res.* **2011,** *44*, 947.
37. R. Vankayala, Y.-K. Huang, P. Kalluru, C.-S. Chiang, K.C. Hwang, *Small* **2014,** *10*, 1612.
38. S. Wang, K.-J. Chen, T.-H. Wu, H. Wang, W.-Y. Lin, M. Ohashi, P.-Y. Chiou, H.-R. Tseng, *Angew. Chem., Int. Ed.* **2010,** *49*, 3777.
39. X. Huang, I.H. El-Sayed, W. Qian, M.A. El-Sayed, *J. Am. Chem. Soc.* **2006,** *128*, 2115.
40. Z. Zhang, L. Wang, J. Wang, X. Jiang, X. Li, Z. Hu, Y. Ji, X. Wu, C. Chen, *Adv. Mater.* **2012,** *24*, 1418.
41 J. Song, L. Pu, J. Zhou, B. Duan, H. Duan, *ACS Nano* **2013,** *7*, 9947.
42. T.S. Hauck, T.L. Jennings, T. Yatsenko, J.C. Kumaradas, W.C.W. Chan, *Adv. Mater.* **2008,** *20*, 3832.
43. C. Ungureanu, R. Kroes, W. Petersen, T.A.M. Groothuis, F. Ungureanu, H. Janssen, F.W.B. van Leeuwen, R.P.H. Kooyman, S. Manohar, van Leeuwen, T. G. *Nano Lett.* **2011,** *11*, 1887-1894.
44. R. Guo, L. Zhang, H. Qian, R. Li, X. Jiang, B. Liu, *Langmuir* **2010,** *26*, 5428.
45. S. Shen, H. Tang, X. Zhang, J. Ren, Z. Pang, D. Wang, H. Gao, Y. Qian, X. Jiang, W. Yang, *Biomaterials* **2013,** *34*, 3150.
46. Z. Xiao, C. Ji, J. Shi, E.M. Pridgen, J. Frieder, J. Wu, O.C. Farokhzad, *Angew. Chem., Int. Ed.* **2012,** *51*, 11853.
47. A.M. Alkilany, L.B. Thompson, S.P. Boulos, P.N. Sisco, C.J. Murphy, *Adv. Drug Delivery Rev.* **2012,** *64*, 190.
48. X. Wang, M. Shao, S. Zhang, X. Liu, *J. Nanoparticle Res.* **2013,** *15*, 1.
49. Y. Chen, Y. Pang, J. Wu, Y. Su, J. Liu, R. Wang, B. Zhu, Y. Yao, D. Yan, X. Zhu, Q. Chen, *Langmuir* **2010,** *26*, 9011.
50. A.J. Mieszawska, Y. Kim, A. Gianella, I. van Rooy, B. Priem, M.P. Labarre, C. Ozcan, D.P. Cormode, A. Petrov, R. Langer, O.C. Farokhzad, Z. A. Fayad, W.J.M. Mulder, *Bioconjugate Chem.* **2013,** *24*, 1429.
51. D.W. Bartlett, M.E. Davis, *Bioconjugate Chem.* **2007,** *18*, 456.
52. N.C. Bellocq, S.H. Pun, G.S. Jensen, M.E. Davis, *Bioconjugate Chem.* **2003,** *14*, 1122.
53. S.H. Pun, N.C. Bellocq, A. Liu, G. Jensen, T. Machemer, E. Quijano, T. Schluep, S. Wen, H. Engler, J. Heidel, M.E. Davis, *Bioconjugate Chem.* **2004,** *15*, 831.
54. S. Tamesue, Y. Takashima, H. Yamaguchi, S. Shinkai, A. Harada, *Angew. Chem., Int. Ed.* **2010,** *49*, 7461.
55. N.A. Merrill, M. Sethi, M.R. Knecht, *ACS Appl. Mater. Interfaces* **2013,** *5*, 7906.
56. T.K. Sau, C.J. Murphy, *Langmuir* **2004,** *20*, 6414.
57. D. Gentili, G. Ori, M. Comes Franchini, *Chem. Commun.* **2009**, 5874.
58. H. Wondraczek, T. Heinze, *Macromol. Biosci.* **2008,** *8*, 606.
59. D. Pacardo, B. Neupane, G. Wang, Z. Gu, G. Walker, F.S. Ligler, *Anal. Bioanal. Chem.* **2015,** *407*, 719.
60. A.B. Lowe, *Polymer Chem.* **2010,** *1*, 17.
61. K. Peng, I. Tomatsu, A. Kros, *Chem. Commun.* **2010,** *46*, 4094.
62. J.M. Rosenholm, A. Meinander, E. Peuhu, R. Niemi, J.E. Eriksson, C. Sahlgren, M. Lindén, *ACS Nano* **2008,** *3*, 197.
63. J.M. Saul, A. Annapragada, J.V. Natarajan, R.V. Bellamkonda, *J. Control. Release* **2003,** *92*, 49.
64. C. Sun, R. Sze, M. Zhang, *J. Biomed. Mater. Res.-A* **2006,** *78A*, 550.
65. Z. Gu, M. Yan, B. Hu, K.-I Joo, A. Biswas, Y. Huang, Y. Lu, P. Wang, Y. Tang, *Nano Lett.* **2009,** *9*, 4533.